Biomaterials 34 (2013) 209–216

Contents lists available at SciVerse ScienceDirect

Biomaterials

journal homepage: www.elsevier.com/locate/biomaterials

CT/fluorescence dual-modal nanoemulsion platform for investigating atherosclerotic plaques

Jiali Ding [a,1], Yuehua Wang [a,1], Ming Ma [a], Yu Zhang [a,*], Shanshan Lu [b], Yanni Jiang [b], Chunmei Qi [c], Shouhua Luo [a], Ge Dong [a], Song Wen [d], Yanli An [d], Ning Gu [a,*]

[a] State Key Laboratory of Bioelectronics, Jiangsu Key Laboratory for Biomaterials and Devices, School of Biological Science and Medical Engineering, Southeast University, Nanjing 210096, PR China
[b] Department of Radiation, The First Affiliated Hospital of Nanjing Medical University, Nanjing 210029, PR China
[c] Department of Cardiology, Xuzhou Medical College Second Affiliated Hospital, Xuzhou 221006, PR China
[d] Jiangsu Key Laboratory of Molecular Imaging and Functional Imaging, Medical School, Southeast University, Nanjing 210009, PR China

ARTICLE INFO

Article history:
Received 26 August 2012
Accepted 14 September 2012
Available online 12 October 2012

Keywords:
QDs-iodinated oil nanoemulsion
Atherosclerotic plaques
Macrophage
CT imaging
Fluorescence imaging

ABSTRACT

Macrophages have become widely recognized as a key target for atherosclerosis imaging, since they contribute significantly to the progression of atherosclerosis. Dual-modal imaging contrast agents with unique X-ray computed tomography (CT) and optical imaging capabilities have great potential in disease diagnosis because of complementary combination of the high spatial resolution of CT with the high sensitivity of optical imaging. Here, a kind of quantum dots (QDs)-iodinated oil nanoemulsion of 80 nm was developed as a CT/fluorescence dual-modal contrast agent. Hydrophobic QDs were embedded in iodinated oil, which subsequently dispersed in water to form the oil-in-water nanoemulsion. The morphology and hydrodynamic size of the nanoemulsion were characterized, CT values and fluorescence properties were detected. Its cytotoxicity and affinity to three different cells were determined in vitro by MTT assay. In vitro Micro-CT and confocal microscopy cell imaging ability of the nanoemulsion were confirmed by co-incubating with murine macrophage cells and human liver cells. Then in vivo accumulation of this nanoemulsion in macrophages in atherosclerotic rabbits was investigated with clinic CT and fluorescence imaging. The results not only indicated the nanoemulsion could be served as a dual-modal contrast agent, but revealed it could specifically target to macrophages and visualize atherosclerotic plaques.

1. Introduction

Recently, researchers have been focused on nanoscale contrast agent which brings significant impact for potential applications in medical diagnosis. The newly developed nanomaterials like magnetic iron oxide nanoparticles, gold nanoparticles and fluorescence quantum dots (QDs), have extraordinary features such as long blood circulation time, target specificity and biocompatibility, as well as excellent contrast enhancement capabilities for magnetic resonance imaging (MRI), X-ray computed tomography (CT) and optical imaging. Current imaging modalities include MRI, CT, positron emission tomography (PET), optical and ultrasound imaging. Each modality can't provide complementary information due to their inherent limitation. Therefore, it is desirable to combine different imaging modalities into one single nanomaterial. With development of nanocomposite technology, multifunctional nanomaterial-based platforms have been constructed as multimodal imaging contrast agents to compensate for the deficiencies of single imaging modality [1–9]. For example, ^{64}Cu labeled magnetofluorescent nanoparticles were yielded for PET/MRI/optical trimodal imaging [10]. Soybean oil nanoemulsion in water loaded with Cy7 and iron oxide nanocrystals represented a nanoparticle platform for MRI/optical imaging [11].

CT is one of the most reliable and widely used diagnostic tools in hospital due to different X-ray absorption of tissue and lesion. Because of the increasing number of detectors and faster rotation speed, the temporal and spatial resolutions of CT scanner are improving [12,16]. Clinical contrast agents for CT contrast enhancement are based on iodinated molecules and compounds with high X-ray absorption coefficient, which will increase visibility in the administrated area of the body. But these contrast agents are

* Corresponding authors. Tel.: +86 25 8327 2496x8005; fax: +86 25 8379 2460.
E-mail address: zhangyu@seu.edu.cn (Y. Zhang).
[1] These authors contributed equally to this work.

0142-9612/$ – see front matter © 2012 Elsevier Ltd. All rights reserved.
http://dx.doi.org/10.1016/j.biomaterials.2012.09.025

small molecules and nonspecific compounds, they will rapidly eliminate from blood vessels and/or lymphatic vessels uptake after an intravenous injection [12–16]. Thus, traditional CT contrast agents are not suitable to image specific organs and diseases. It is necessary to encapsulate CT contrast agents into various nanoparticulate carriers, such as nanoemulsion and liposome [11,17–24] to overcome these disadvantages. Slowed diffusion into extravascular space or decreased renal clearance allows adequate time for accumulation in lesions, resulting in high efficiency and specificity of distribution [13].

On the other hand, nanometer-sized semiconductor particles (quantum dots, QDs) with unique photochemical and photophysical are of considerable interest in many research areas, they can be covalently linked to peptides, antibodies, nucleic acids or small molecule ligands as fluorescent probes [25–29]. Fluorescent quantum dots have higher levels of brightness and photo-stability compared with conventional organic fluorophores, and are well suited for optical encoding and multiplexing applications due to their broad excitation profiles and narrow/symmetric emission spectra. The new generations of quantum dots have far-reaching potential for the study of intracellular processes at the single-molecule level, high-resolution cellular imaging, long-term in vivo observation of cell trafficking, tumor targeting and diagnostics [30,31].

In short, CT as a powerful diagnostic tool has high spatial resolution, short imaging time and three-dimensional (3D) imaging but suffers from low target sensitivity. Large doses of small iodinated molecule agents (tens of grams) are typically needed to provide adequate contrast, which sometimes cause adverse reactions for patients. Optical probes have relatively good sensitivity, but it is limited by low tissue penetration depths [8,32]. Therefore, incorporation of fluorescent species like QDs into iodine contained nanoemulsion can create a dual-modal contrast agent, providing combined advantages of CT and optical imaging. Moreover, this agent can be functionalized to increase blood circulation times and to endow target specificity, with a larger time window for imaging and enhanced imaging contrast at permissible dose [9,33]. This nanomaterial platform is based on oil-in-water emulsion carrying both a high payload of hydrophobic material and a hydrophilic material in surfactant corona [4,22,23]. Herein, we developed such kind of all-in-one nanomaterial which is easily synthesized and functionalized, and then explored for its potentials as a dual-modal contrast agent for both CT/optical imaging. It is composed of a hydrophobic iodinated oil core component containing QDs inside, the oil droplets are stabilized by a mixed surfactant that favors the formation of small nanoparticles. PEGylated lipids used in this synthesis can prominently improve the circulation time [34], so more droplets will accumulate in macrophages in atherosclerotic plaques to provide a better contrast effect. A series of comprehensive evaluations are performed to characterize their size, morphology, cytotoxicity, CT/fluorescence imaging effects in vitro and vivo.

2. Materials and methods

2.1. Materials

Polyoxyethylene glycol monostearate (Aladdin), Core/shell CdSe/ZnS QDs in hexane (8 μM, WUHAN JIAYUAN QUANTUM DOTS CO., LTD), Iodinated oil injection (Guerbet, France), Lipoid E-80 (Lipoid, German), MTT solution (KeyGEN Biotech, China), Distilled water.

2.2. Synthesis of oil-in-water nanoemulsion

100 mg Lipoid E-80 was dissolved in 200 μl ethanol. 500 μl core-shell CdSe/ZnS QDs dispersed in hexane with an emission wavelength at about 625 nm was mixed with 500 μl Iodinated oil injection, then heated in water bath to remove hexane. These two parts made up the oil phase. 180 mg Polyoxyethylene glycol monostearate was dissolved in 20 ml distilled water which served as water phase. Subsequently, the oil phase was added dropwise under continuous stirring to boiling water phase. The preparation was concentrated to 10 ml and the crude emulsion was sonicated under probe ultrasonication for 15 min (Sonics, VCX750). The final nanoemulsion was stored in the dark at 4 °C.

2.3. Transmission electron microscopy

A JEM-2100 electron microscope (JEOL) with a working voltage of 200 kV was used to observe the morphology of the nanoemulsion. Transmission electron microscopy (TEM) image negatively stained by 2% sodium phosphotungstate (PH = 7.0) was taken from the 1:10 diluted nanoemulsion [35].

2.4. Dynamic light scattering

A dynamic light scattering (DLS) device from Malvern Instruments (mode) was used to measure the hydrodynamic size of the nanoemulsion. Before the measurement, 30 μl nanoemulsion was diluted with 3 ml distilled water.

2.5. In vitro CT imaging

The nanoemulsion with different concentration were imaged by a clinical 64-slice multidetector CT scanner (SOMATOM Emotion, Siemens, German). Iodinated oil injection and distilled water were set as two controls. The six samples were imaged with following parameters: tube voltage, 130 kV; current intensity, 180 mAs; slice thickness, 5.0 mm; scan time, 2.85 s.

2.6. In vitro fluorescence imaging

We performed the ex vivo fluorescence imaging of the QDs-iodinated oil nanoemulsion with total internal reflection fluorescence microscopy (TIRFM) model. A iXon + DU 897 EMCCD (Audor) camera was mounted on top of a Nikon Ti-E microscope with a 100× oil type objective (1.49 NA). To detect the fluorescence of the QDs (emission wavelength is 625 nm), a 491 nm excitation filter and a 600–637 nm emission filter were used.

On the other hand, the emission spectrum of the QDs-iodinated oil nanoemulsion was measured using a Hitachi F-7000 fluorescence spectrometer equipped with a xe lamp under a working voltage of 400 V. The emission slits was set at 10.0 nm and scanning speed was 1200 nm/min. Excitation wavelength was 500 nm.

2.7. Cell culture

Human liver cell line (HL7702 cells), human hepatoma cell line (HepG2 cells) and murine macrophage cell line (RAW264.7 cells) were cultured in PRMI-1640 medium supplemented with 10% FBS and 1% penicillin-streptomycin at 37 °C and 5% CO_2 in a humidified incubator.

2.8. In vitro cytotoxicity (MTT assay)

HL7702 cells, HepG2 cells and RAW264.7 cells in PRMI-1640 were added into each well in a 96-well plate and incubated for 24 h. The culture medium was replaced by fresh medium containing different concentrations of the nanoemulsion ranging from 7.5 to 240 μg/ml (iodine concentration) for 24 h. After washing the cells twice with serum-free medium, 150 μl serum-free medium was added to each well followed by MTT solution. The cells were then incubated at 37 °C for 4 h, the medium was slightly taken away and 150 μl DMSO was added. The optical density (OD_{sto}) was measured at 570 nm with a microplate reader (BIO-RAD, model 680).

2.9. In vitro micro-CT imaging of cells

RAW264.7 cells were incubated with the QDs-iodinated oil nanoemulsion 600 μg/ml (iodine concentration) for 8 h at 37 °C. After washed with PBS buffer for three times, cells were trypsinized and centrifuged at 1000 rpm for 5 min to wash out unendocytosed nanoemulsion, then the cells were placed in a 1.5 ml Eppendorf tube. Every tube was hold in place using a styrofoam and scanned by a micro-CT imaging system (Hiscan MCT-1108, HEJUN, Suzhou) with the following parameters: tube voltage, 40 kV; current intensity, 120 mAs. Images were reconstructed on the micro-CT system workstation Hiscan (HEJUN, Suzhou) using the 3D data analysis mode.

2.10. In vitro optical imaging of cells

The cellular uptake and the intracellular fluorescence were followed with confocal laser scanning microscopy (LSCM, Olympus, Ox81, F1000) using HL7702 cells and RAW264.7 cells. The cells were incubated in 24-well plates (1×10^3 cells/well) with the QDs-iodinated oil nanoemulsion for 24 h. The medium was removed, the cells were washed twice with serum-free medium. Then the cells were stained with DAPI before placed on glass slides. The optical contrast effect was analyzed with LSCM.

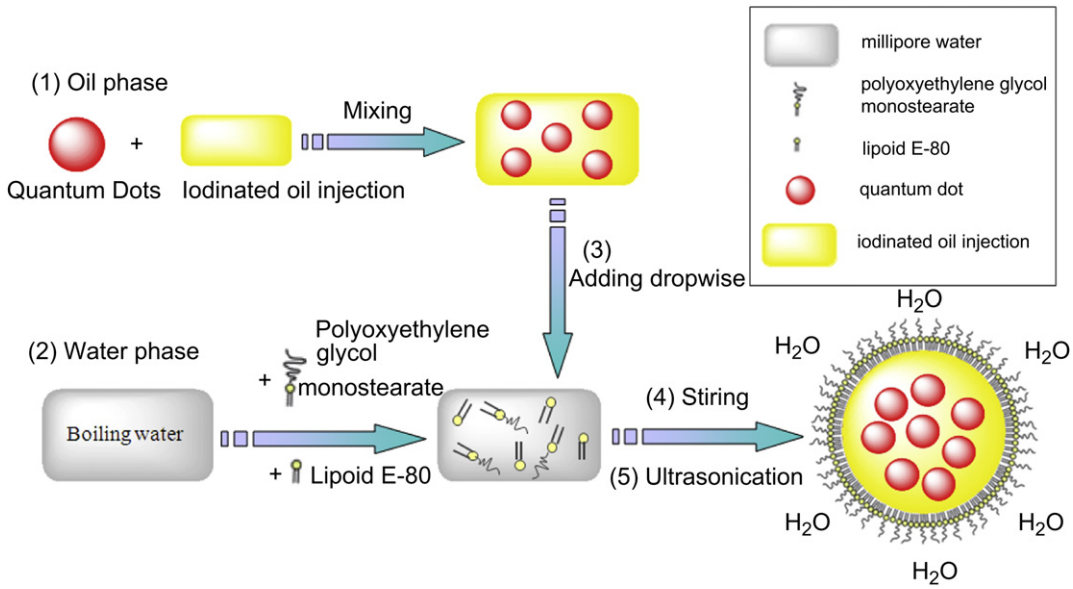

Fig. 1. Schematic representation of the nanoemulsion formation process in this study. (1) Core/shell CdSe/ZnS QDs dispersed in hexane was mixed with iodinated oil, hexane is evaporated by heating the mixture. (2) Different lipids are added to the water, making up the water phase. (3) The mixture of (1) is added dropwise to (2). (4,5) Vigorous stirring and ultrasonication results in an emulsion, with the iodinated oil and QDs enclosed in a lipid layer.

2.11. Animal protocol

All animal experiments were approved and performed in accordance with the Animal Management Rules of the Ministry of Health of the People's Republic of China and the guidelines for the Care and Use of the Southeast University Laboratory Animal Center.

Adult New Zealand White (NZW) male rabbits ($n = 5$) were used for the present study. After balloon-induced endothelial injury in the abdominal aorta, three rabbits were fed a high-cholesterol diet containing 1% cholesterol for ten weeks [48], which were conducted by Xuzhou Medical College Second Affiliated Hospital. Two rabbits were used as controls and only fed high cholesterol diet.

2.12. In vivo distribution of the QDs-iodinated oil nanoemulsion and detection of macrophages in atherosclerotic plaques by CT imaging

Atherosclerotic rabbits were scanned by a clinical CT (SOMATOM Emotion, Siemens, German) to estimate the in vivo CT efficacy of the nanoemulsion due to nonspecific uptake of nanoparticles in plaques. After pre-scans, three rabbits were intravenously injected with the nanoemulsion (100 mg iodine/kg body weight) and scanned at several time points postinjection (10 s, 5 min, 30 min, 1 h, 1.5 h, 2 h). All scans were accomplished with following parameters: tube voltage, 130 kV; current intensity, 25 mAs; abdomen abdmultiphase sequence.

2.13. Near-infrared fluorescence (NIRF) imaging of excised aortas

From the previous CT studies, we estimated the optimal imaging time for the detection of macrophages in atherosclerotic plaques to be 2 h after administration. Hence, We sacrificed the rabbits before and 2 h after injection with the nanoemulsion. Their aortas were removed after perfusion and imaged with a fluorescence imaging system (Maestro2.10.0, CRI) at a magnification of ×2 and a wavelength of 532 nm.

3. Results and discussion

3.1. Synthesis and characterization of the nanoemulsion

Usually, O/W nanoemulsion contains three parts: water phase, oil phase and surfactant [36]. To synthesize the O/W nanoemulsion, we developed a pretty simple method with good repeatability (Fig. 1). Here, oil phase was added dropwise under vigorous stirring to the boiling water phase consisted of surfactant to form crude emulsion immediately. Subsequently, the emulsion was homogenized using a sonicator tip to form a uniform nanoemulsion.

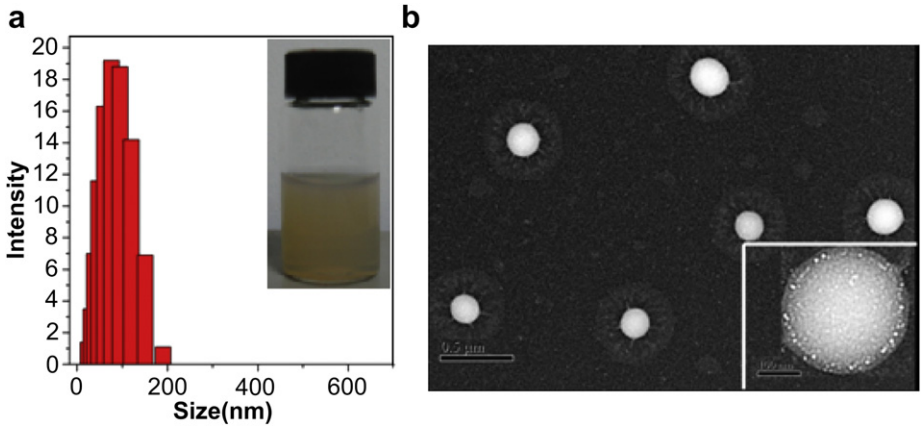

Fig. 2. (a) Dynamic light scattering (DLS) sizes measurement of the QDs-iodinated oil nanoemulsion, Inset: photograph of the nanoemulsion. (b) Negatively stained transmission electron microscopy (TEM) images of the nanoemulsion. Scale bar is 0.5 μm, 100 nm, respectively.

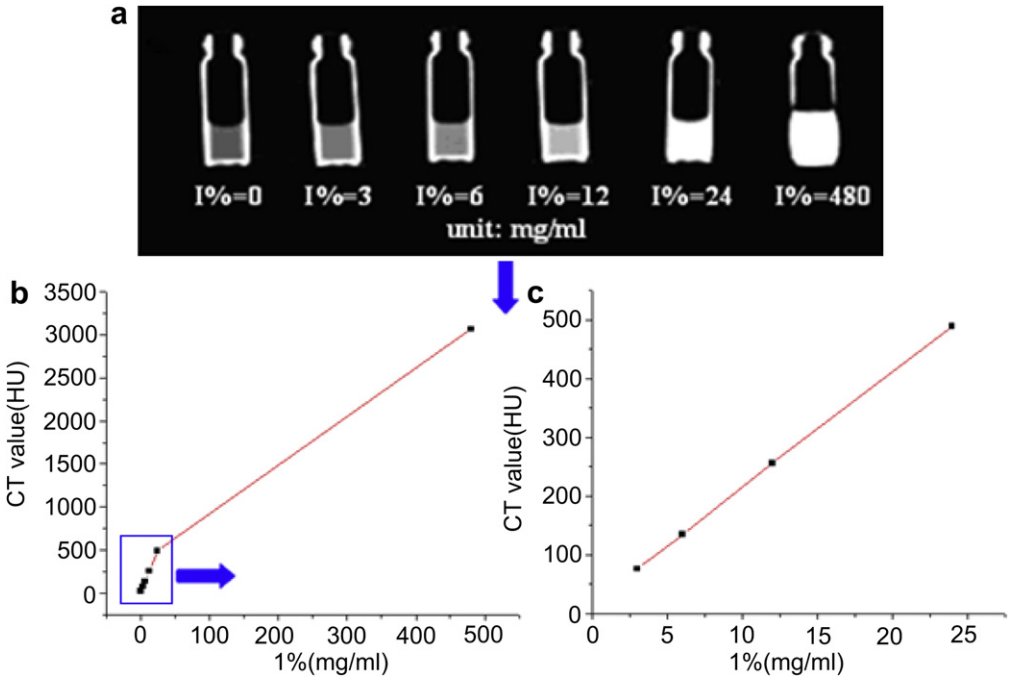

Fig. 3. (a) In vitro CT imaging of the QDs-iodinated oil nanoemulsion with different iodine concentration. (b) The measured CT value of the six samples as a function of iodine concentration. (c) Linear relationship for the four samples.

Sonication was noted as a significant step, which made the droplet smaller and more uniform.

The hydrodynamic mean size of the nanoemulsion was measured by DLS (Fig. 2a). Mean size of the nanoparticle was 81.3 nm with the polydispersity index of 0.21. This small size accommodated nanoparticles uptake by cells [11]. To observe the morphology of the QDs-iodinated nanoemulsion, negative stain transmission electron microscopy was performed (Fig. 2b). The TEM image showed the nanoparticle had a spherical shape with a size of approximately 200 nm. Compared with DLS result, the size was bigger than the hydrodynamic size. This may be when the nanoemulsion were deposited on a TEM cupper grid coated with a holey carbon film, the oil droplets would collapse which made the size bigger. In the photograph showed in Fig. 2a inset, the sample was transparent, which could be explained by small characteristic size of the nanoemulsion [46].

3.2. In vitro CT imaging and fluorescence imaging

In vitro CT imaging property of six samples with different iodine concentration from 0 to 240 mg/ml was studied. The nanoemulsion showed significantly higher CT value than distilled water. Appreciable CT contrast enhancement was observed with different iodine concentration (Fig. 3a). With the increase of iodine concentration, the enhancement consistently increased and densities in HU of six samples were plotted in Fig. 3b. The intensities of the four samples with different iodine concentration has a linear relationship (Fig. 3c). The results indicate that the nanoemulsion's CT contrast enhancement efficiency is dependent on the amount of iodine. The higher concentration of the iodine, the brighter images and higher CT value can be obtained.

Then total internal reflection fluorescence microscopy (TIRFM) and fluorescence spectrometer were used to characterize the

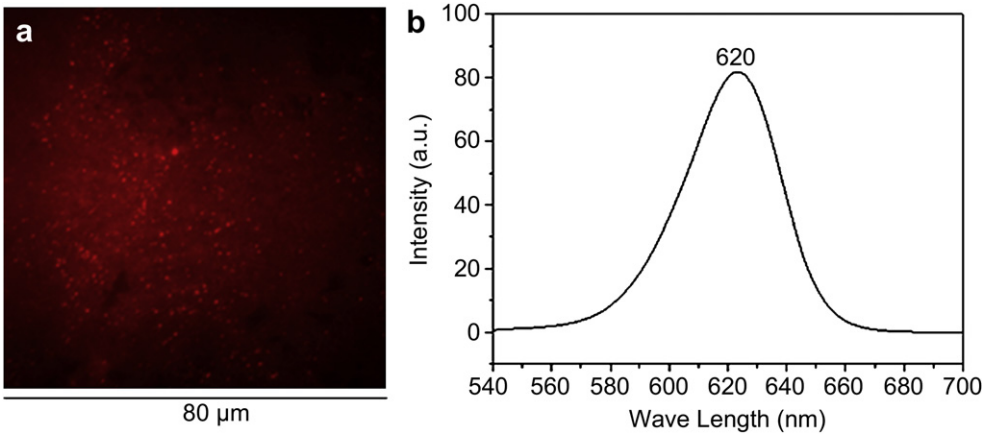

Fig. 4. In vitro fluorescence imaging of the QDs-iodinated oil nanoemulsion. (a) Total internal reflection fluorescence microscopy (TIRFM) image. (b) Fluorescence emission spectrum of the nanoemulsion.

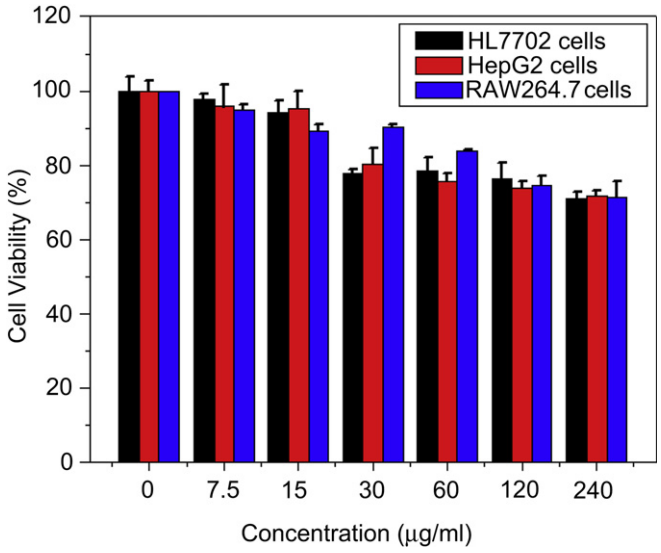

Fig. 5. In vitro cytotoxicity of the QDs-iodinated oil nanoemulsion evaluated by MTT assay, iodine concentration ranges from 7.5 to 240 μg/ml, $^{*}p < 0.05$.

optical properties of the nanoemulsion (Fig. 4a). From TIRFM image, isolated fluorescence dots can be clearly observed, attributed to the emission of QDs in nanoemulsion droplet. In general, QDs' fluorescence can enlarge the size of each droplet due to the point spread function [47], so the observed fluorescence dots display much more size than the hydrodynamic size as described above. In addition, fluorescence spectrum measurement (Fig. 4b) revealed the nanoemulsion was located the same maximum emission wavelength at 620 nm as QDs [23]. It can be concluded that the QDs are imbedded in iodinated oil nanoemulsion and exhibits great potential for CT and optical dual-modal imaging.

3.3. Cytotoxicity and biocompatibility

MTT assay [37] was carried out to evaluate the cytotoxicity of QDs-iodinated oil nanoemulsion in human liver cell line (HL7702 cells), human hepatoma cell line (HepG2 cells) and murine macrophage cell line (RAW264.7 cells). Results (Fig. 5) revealed no significant influence on cell viability was detected at iodine concentration below 30 μg/ml (both HL7702 cells and HepG2 cells viability >90%, RAW264.7 cells was relatively a little higher than the others below 60 μg/ml). When the iodine concentration is above 30 μg/ml, the cell viability reduced but was still above 70%. As demonstrated, the cell viability decreased with the increasing of iodine concentration, and the cell viability had no obvious specific relationship with cell type used.

3.4. In vitro CT imaging and optical imaging of cells

The nanoemulsion containing QDs could enter into cells because of endocytosis [38]. HL7702 and RAW264.7 cells were incubated

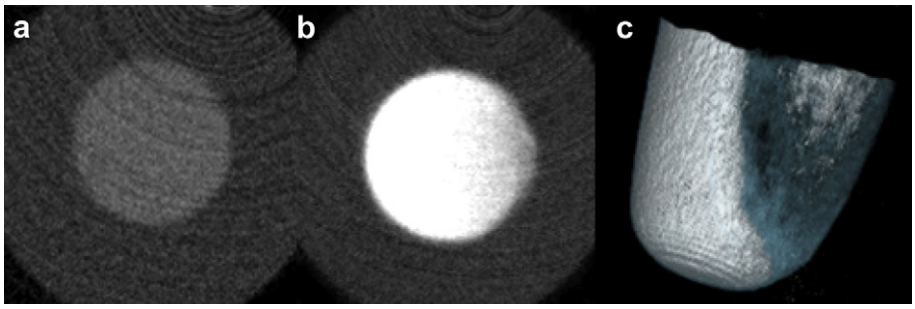

Fig. 6. Transection micro-CT images of RAW264.7 cell mass incubated with culture medium (a) and the QDs-iodinated oil nanoemulsion (b) for 8 h. (c) The 3D display of (b).

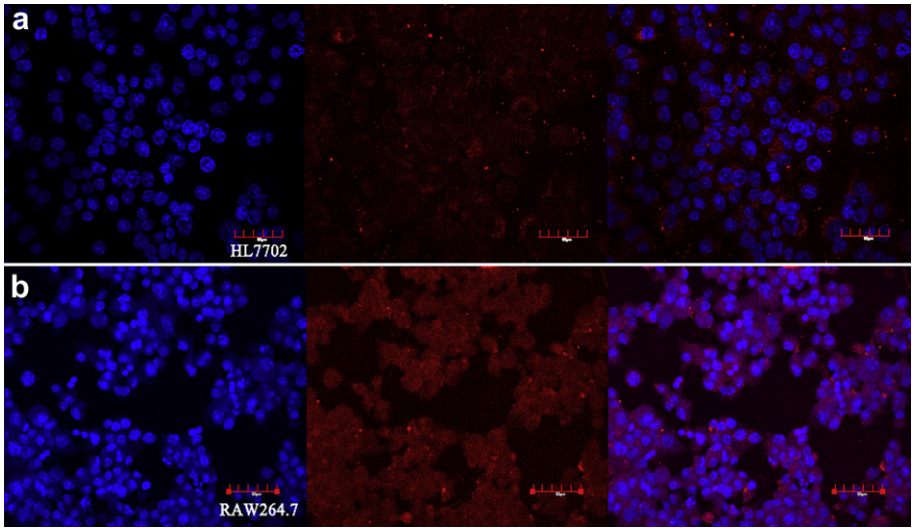

Fig. 7. LSCM images of (a) HL7702 cells and (b) RAW264.7 cells incubated with the QDs-iodinated oil nanoemulsion (Iodine concentration was 120 μg/ml). Images from left to right show nuclei stained by DAPI (blue), nanoemulsion fluorescence (red) and the overlay of two images. The scale bars are 50 μm in all images. (For interpretation of the references to color in this figure legend, the reader is referred to the web version of this article.)

with the QDs-iodinated oil nanoemulsion to assess the intracellular CT and fluorescence imaging property.

To investigate in vitro CT efficacy, RAW264.7 cells incubated at iodine concentration of 600 μg/ml for 8 h were imaged using a micro-CT imaging system. Fig. 6(a, b) showed the transection CT images of the cell mass with or without (as blank control) incubation of the nanoemulsion. It was clear that the incubated cell mass were brighter than blank control cell mass. The acquired

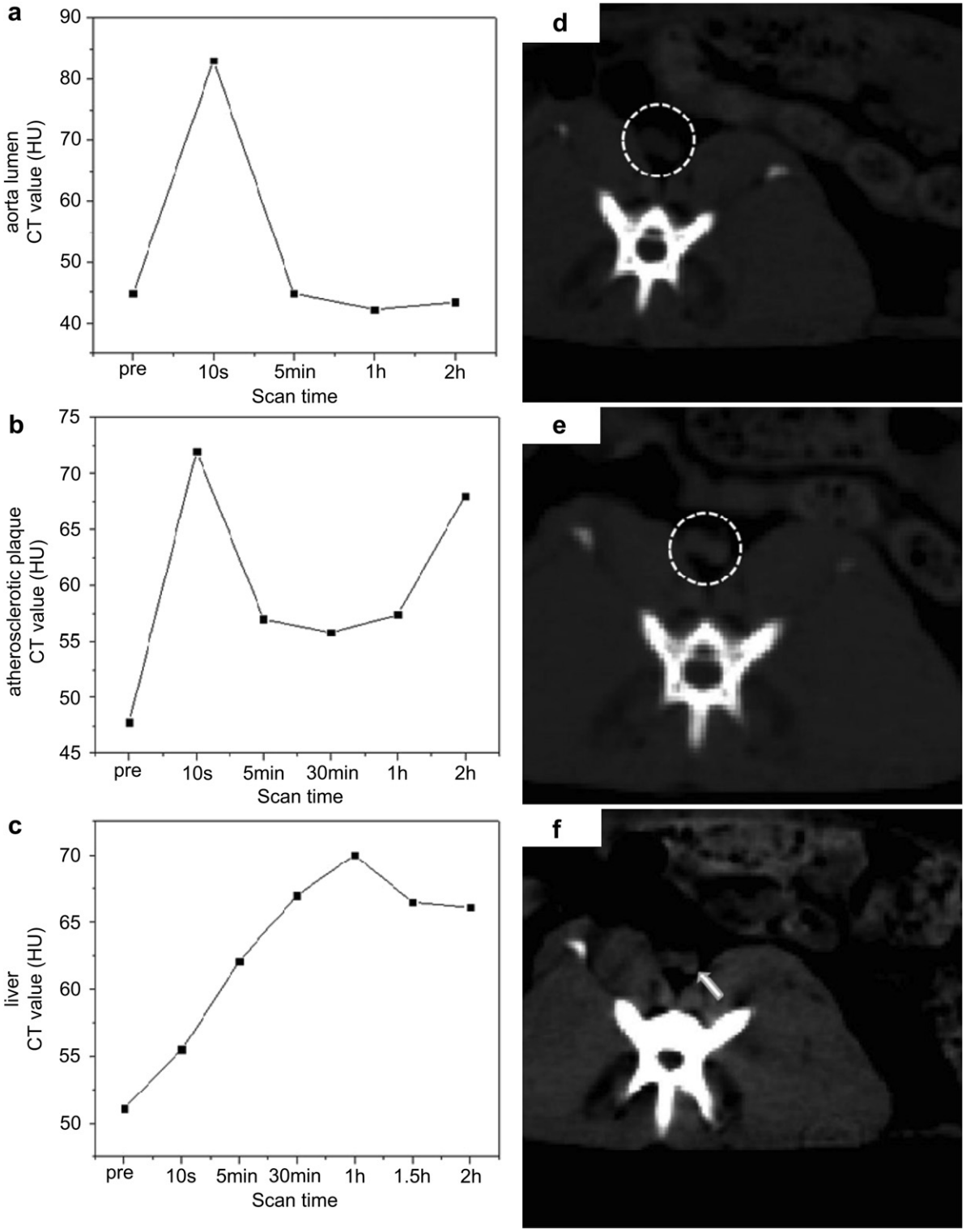

Fig. 8. Kinetics and distribution of QDs-iodinated oil nanoemulsion in atherosclerotic rabbits. (a, b, c) CT values of different organs for pre-injection and at different time points for postinjection of the nanoemulsion. (a) aortas lumen; (b) atherosclerotic plaques, showing the atherosclerotic plaques were significantly higher 2 h postinjection; (c) liver. (d, e, f) CT images of the abdominal aorta (white circle) of NZW rabbit, the atherosclerotic plaques were indicated by arrows. (d) before; (e) 10 s and (f) 2 h after the injection of QDs-iodinated oil nanoemulsion. Before injection, the atherosclerotic plaques could not be differentiated from the surrounding tissues, whereas a strong enhancement was detected in the plaques 2 h after the injection of the nanoemulsion.

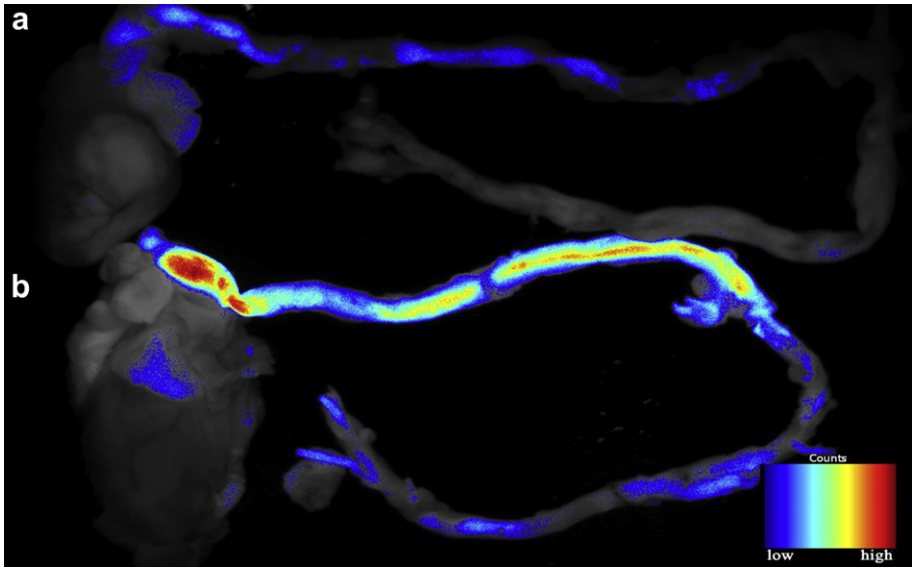

Fig. 9. Fluorescence imaging of excised aortas with QDs-iodinated oil nanoemulsion. The whole aortas were excised (a) without injection of the nanoemulsion; (b) 2 h after the injection. The signal intensity was significantly higher in the atherosclerotic plaques, meaning the accumulation of the nanoemulsion.

images in Digital Imaging and Communications in Medicine (DICOM) format of incubated cell mass were 3D reconstructed using Hiscan software (Fig. 6(c)).

HL7702 and RAW264.7 cells' fluorescence imaging effects were displayed using confocal laser scanning microscopy (LSCM) (Fig. 7). DAPI (4′, 6-diamidino-2-phenylin-dole), a kind of DNA-specific probe, can enter into cells, attach in the minor grove of A–T rich sequences of DNA and form a blue fluorescent complex [39]. The blue dots excited at 408 nm represented nucleus in the cells, and the areas were red due to the fluorescence from QDs with excitation wavelength 488 nm. Both HL7702 and RAW264.7 cells can endocytose QDs-iodinated oil nanoemulsion and generate intracellular fluorescence, the nanoemulsion mainly accumulated in the cytoplasm. The fluorescence intensity from RAW264.7 cells was stronger than HL7702 cells, suggesting macrophages could endocytose more nanoemulsion.

In brief, the QDs-iodinated oil nanoemulsion is capable of becoming a CT/optical dual-modal probe for cell imaging.

3.5. In vivo distribution and detection of macrophages in atherosclerotic plaques via CT and near-infrared fluorescence (NIRF)

High levels of macrophage infiltration existed in atherosclerotic plaques plays a vital role in the progression of atherosclerosis [40]. As a result, macrophages have been identified as a key biological marker of vulnerable plaques [10,41–45]. In this experiment, atherosclerotic rabbits were used to detect macrophages with CT after administration of the nanoemulsion. This model has been widely used to study the effects of contrast agents on atherosclerotic plaques due to its high levels of macrophage infiltration and similar to human coronary atherosclerotic plaques [41]. After ear vein injection of the nanoemulsion, serial CT imaging of the rabbits was performed to observe the enhancement in the blood and macrophage-rich tissues such as liver and atherosclerotic plaques to detect the macrophage infiltration. Furthermore, we tested if the nanoemulsion could passively target the macrophages in atherosclerotic plaques.

The change of X-ray absorption value (CT value) in aortic lumen, atherosclerotic plaques and liver was showed in Fig. 8. 10 s after administration, the CT imaging of aortic lumen was rapidly enhanced (Fig. 8d, e), the CT value of aortic lumen was 83 ± 1.3 HU compared to 44.8 ± 3.5 HU pre-injection, but the vascular enhancement decreased quickly, CT value in aortic lumen declined to pre-injection value, As time went by, the nanoemulsion began targeting to macrophage-rich areas. Thus 2 h after administration, CT value in atherosclerotic plaques was significantly different from pre-injection value (68.0 ± 3.1 HU versus 44.8 ± 3.5 HU), whereas there was no significant difference of CT value in aortic lumen (Fig. 8a, b). At this point, the enhancement of atherosclerotic plaques and aortic lumen in CT images could be discriminated (Fig. 8f). CT values measured in liver reached highest 1 h after administration (70.0 ± 1.9 HU versus 51.1 ± 2.2 HU), then slowly decreased with metabolism (Fig. 8c). The achieved enhancement was about 20 Hu when employing an injection dose of 100 mg/kg body weight of the nanoemulsion. This is comparable with the enhancement (14 Hu) reported in the literature using iodinated nanoparticulate contrast agent N1177 with a hydrodynamic size of 259 nm [45], but in which a much more injection dose of 250 mg/kg body weight was adopted. That is, with much smaller doses, the nanoemulsion can reach the same signal enhancement. The reason may be that our nanoemulsion has smaller size, which can avoid the phagocytose by the reticuloendothelial system (RES) and lead to more accumulation in macrophage-rich organs.

Next, the aortas of rabbits were excised and scanned using a near-infrared fluorescence imaging system to estimate uptake of the nanoemulsion in aortas. The aortic arch and the abdominal aorta had higher signal intensity, meaning these segments were plaque-loaded areas (Fig. 9).

Accordingly, it is further demonstrated the QDs-iodinated oil nanoemulsion has a great potential targeting to macrophage-rich region to evaluate atherosclerosis with CT/fluorescence imaging.

4. Conclusion

A method for establishing an 80 nm oil-in-water nanoemulsion platform is developed for both CT and fluorescent imaging. The nanoemulsion is composed of QDs in iodinated oil stabilized by PEGylated lipids, and it is demonstrated that this nanoemulsion has good fluorescence and X-ray absorption abilities making it efficient optical/CT contrast enhancement for cell imaging. Further studies

show the nanoemulsion has great potential of targeting and visualizing atherosclerotic plaques with uptake in vivo by macrophages. These results indicate this nanoemulsion can serve as a dual-modal CT/fluorescence contrast agent and holds great potential for future application.

Acknowledgment

This research was supported by the National Important Science Research Program of China (No. 2011CB933503, 2013CB733800), National Natural Science Foundation of China (No. 31170959, 30970787, 61127002), the Basic Research Program of Jiangsu Province (Natural Science Foundation, No. BK2011036, BK2009013), and National Key Technology Research and Development Program of the Ministry of Science and Technology of China (2012BAI23B02).

References

[1] Liu Y, Miyoshi H, Nakamura M. Nanomedicine for drug delivery and imaging: a promising avenue for cancer therapy and diagnosis using targeted functional nanoparticles. Int J Cancer 2007;120:2527–37.
[2] Cormode DP, Skajaa T, Fayad ZA, Mulder WJ. Nanotechnology in medical imaging probe design and applications. Arterioscler Thromb Vasc Biol 2009; 29:992–1000.
[3] Mulder WJM, Strijkers GJ, Van Tilborg GAF, Cormode DP, Fayad ZA, Nicolay K. Nanoparticulate assemblies of amphiphiles and diagnostically active materials for multimodality imaging. Acc Chem Res 2009;42:904–14.
[4] Gao JH, Gu HW, Xu B. Multifunctional magnetic nanoparticles: design, synthesis, and biomedical applications. Acc Chem Res 2009;42:1097–107.
[5] Kim J, Piao Y, Hyeon T. Multifunctional nanostructured materials for multimodal imaging and simultaneous imaging and therapy. Chem Soc Rev 2009; 38:372–90.
[6] Weissleder R, Mahmood U. Molecular imaging. Radiology 2001;219:316–33.
[7] Peer D, Karp JM, Hong S, Farokhzad OC, Margalit R, Langer R, et al. Nanocarrier as an emerging platform for cancer therapy. Nat Nanotechnol 2007;2:751–60.
[8] Cheon J, Lee JH. Synergistically integrated nanoparticles as multimodal probes for nanobiotechnology. Acc Chem Res 2008;41:1630–40.
[9] Angelique L. Multimodality imaging probes: design and challenges. Chem Rev 2010;110:3146–95.
[10] Matthias N, Hanwen Z, Sheena H, Peter P, David ES, Elena A, et al. Nanoparticle PET-CT imaging of macrophages in inflammatory atherosclerosis. Circulation 2008;117:379–87.
[11] Anita G, Peter AJ, Venkatesh M, Sarayu R, Claudia C, Jun T, et al. Multifunctional nanoemulsion platform for imaging guided therapy evaluated in experimental cancer. ACSNano 2011;5:4422–33.
[12] Chou SW, Shau YH, Wu PC, Yang YS, Shieh DB, Chen CC. In vitro and in vivo studies of FePt nanoparticles for dual modal CT/MRI molecular imaging. J Am Chem Soc 2010;132:13270–8.
[13] Dongkyu K, Sangjin P, Jae HL, Yong Y, Sangyong J. Antibiofouling polymer-coated gold nanoparticles as a contrast agent for in vivo x-ray computed tomography imaging. J Am Chem Soc 2007;129:7661–5.
[14] Rutten A, Prokop M. Contrast agents in x-ray computed tomography and its applications in oncology. Anticancer Agents Med Chem 2007;7:307–16.
[15] Pachela P, Ashish A, Nicholas AK, Aron P. Targeted gold nanoparticles enable molecular CT imaging of cancer. Nano Lett 2008;8:4593–6.
[16] Teng L, Peng H, Guo G, Shen G, Fu S, Cui DX, et al. Mesoporous silica-coated gold nanorods with embedded indocyanine green for dual mode X-ray CT and NIR fluorescence imaging. Opt Express 2011;19:17030–9.
[17] Francois H, Nicolas A, Guy Z, Philippe C, Xiang L, Youri A, et al. Radiopaque iodinated nano-emulsions for preclinical X-ray imaging. RSV Adv 2011;1: 792–801.
[18] Alexander TY, Adriana LL, Eric KW, Mary JC, Nicholas P. Novel iodinated dendritic nanoparticles for computed tomography imaging. Nano Lett 2002;2: 595–9.
[19] Kweon S, Lee HJ, Hyung WJ, Suh J, Lim JS. Liposomes coloaded with iopamidol/lipiodol as a RES-targeted contrast agent for computed tomography imaging. Pharm Res 2010;27:1408–15.
[20] Kong WH, Lee WJ, Cui ZY, Bae KH, Park TG, Kim JH, et al. Nanoparticulate carrier containing water-insoluble iodinated oil as a multifunctional contrast agent for computed tomography imaging. Biomaterials 2007;28: 5555–61.
[21] DeKrafft KE, Xie Z, Cao G, Tran S, Ma L, Zhou OZ, et al. Iodinated nanoscale coordination polymers as potential contrast agents for computed tomography. Angew Chem Int Ed 2009;48:9901–4.
[22] Peter AJ, Torjus S, Anita G, David PC, Daniel DS, Stephen DD, et al. Iron oxide oil-in-water emulsions as a multifunctional nanoparticle platform for tumor targeting and imaging. Biomaterials 2009;30:6947–54.
[23] Rolf K, Matti M, Jan H, Karolien C, David PC, Gustav JS, et al. Paramagnetic lipid-coated silica nanoparticles with a fluorescent quantum dot core: a new contrast agent platform for multimodality imaging. Bioconjug Chem 2008;19: 2471–9.
[24] Michael D, Jinzi Z, Rosenblat J, Jaffray DA, Allen C. APN/CD13-targeting as a strategy to alter the tumor accumulation of liposomes. J Control Release 2011;154:298–305.
[25] Bruchez M, Moronne M, Gin P, Weiss S, Alivisatos AP. Semiconductor nanocrystals as fluorescent biological labels. Science 1998;281:2013–5.
[26] Chan WCW, Nie SM. Quantum dot bioconjugates for ultrasensitive nonisotopic detection. Science 1998;281:2016–8.
[27] Michalet X, Pinaud FF, Bentolila LA, Tsay JM, Doose S, Li JJ, et al. Quantum dots for live cells, in vivo imaging, and diagnostics. Science 2005;307:538–44.
[28] Medintz IL, Uyeda HT, Goldman ER, Mattoussi H. Quantum dot bioconjugates for imaging, labeling and sensing. Nat Mater 2005;4:435–46.
[29] Bailey RE, Smith AM, Nie SM. Quantum dots in biology and medicine. Physica E 2004;25:1–12.
[30] Alivisatos AP. Perspectives on the physical chemistry of semiconductor nanocrystals. J Phys Chem 1996;100:13226–39.
[31] Alivisatos AP. The use of nanocrystals in biological detection. Nat Biotechnol 2004;72:47–52.
[32] Kelong A, Jianhua L, Qinghai Y, Yangyang H, Lehui L. Large-scale synthesis of Bi_2S_3 nanodots as a contrast agent for in vivo x-ray computed tomography imaging. Adv Mater 2011;23:4886–91.
[33] Matsuura N, Rowlands JA. Towards new functional nanostructures for medical imaging. Med Phys 2008;35:4474–87.
[34] Paul AM, Ahmed MF. Nanomedicine-based cancer targeting: a new weapon in an old war. Nanomedicine (Lond) 2010;5:3–5.
[35] Forte TM, Nordhausen RW. Electron microscopy of negatively stained lipoproteins. Meth Enzymol 1986;128:442–57.
[36] Bouchemal K, Briancon S, Perrier E, Fessi H. Nano-emulsion formation using spontaneous emulsification: solvent, oil and surfactant optimization. Int J Pharm 2004;280:241–51.
[37] Fei L, Dawei D, Xinyang C, Zhiyu Q, Samuel A, Yueqing G. Folate-polyethylene glycol conjugated near-infrared fluorescence probe with high targeting affinity and sensitivity for in vivo early tumor diagnosis. Mol Imaging Biol 2010;12:595–607.
[38] Wr Roger, Murray R, Richard E. Endocytosis in change liver cells. J Cell Biol 1971;50:804–17.
[39] Jan K. DAPI: a DNA-specific fluorescent probe. Biotech Histochem 1995;70: 220–33.
[40] Zhang Z, Machac J, Helft G, Worthley S. Non-invasive imaging of atherosclerotic plaques macrophage in a rabbit model with ^{18}F-FDG PET: a histopathological correlation. BMC Nucl Med 2006;6:3.
[41] Hiaanori K, Sarah PS, Toshiro K, Masahiro T, Joelle KB, Dwight GN, et al. FeCo/graphite nanocrystals for multi-modality imaging of experimental vascular inflammation. PLoS One 2011;6:e14523.
[42] Masahiro T, Masaki U, Hisanori K, Philip ST, Mark JY, Steven MC, et al. Human ferritin cages for imaging vascular macrophages. Biomaterials 2011;32:1430–7.
[43] Wilfredo A, Wei X, Bindu V, Philip SL. Imaging of atherosclerosis in apolipoprotein E knockout mice: targeting of a folate-conjugated radiopharmaceutical to activated macrophages. J Nucl Med 2010;51:768–74.
[44] Benjamin RJ, Bjorn G, David LK, Angelique YL. Synthesis of ^{64}Cu-labeled MNP for multimodal imaging. Bioconjug Chem 2008;19:1496–504.
[45] Fabien H, Jonathan EF, Ronald G, Esad V, Vardan A, Edward AF, et al. Noninvasive detection of macrophages using a nanoparticulate contrast agent for computed tomography. Nat Med 2007;20:636–41.
[46] Solans C, Izquierdo P, Nolla J, Azemar N. Nano-emulsions. Curr Opin Colloid Interface Sci 2005;10:102–10.
[47] Peter JS, David JR. The point-spread function of a confocal microscope: its measurement and use in deconvolution of 3-D data. J Microsc (Oxford) 1991; 163:151–65.
[48] John AR, John WC, Yuanxin C, Amanda MH, Elisenda R, Fred R, et al. Enzyme-sensitive magnetic resonance imaging targeting myeloperoxidase identifies active inflammation in experimental rabbit atherosclerotic plaques. Circulation 2009;120:592–9.